

# Developing a benchmark study for bridge monitoring

Structural health monitoring is the process of implementing a continuous damage detection strategy to optimize the inspection and maintenance schedules of bridges, and extend their lifespans. One of the main challenges of automated damage detection is the lack of data on damaged states, which makes it difficult to validate new approaches in the research and development stage. To alleviate this problem, a monitoring campaign on a two-span test bridge with defined defects is conducted and documented in this article. The bridge is a steel-concrete composite structure with a length of 30 m, with two primary steel girders and a segmented concrete deck. The recorded data capture the long-term ambient data from 18 test days and changing environmental conditions, as well as the short-term ambient data and dynamic load tests from four damage scenarios with well-defined damage extents. A mobile measurement system with numerous sensors is used for data acquisition. A shaker is placed on the bridge to excite white noise. The main goal of this article is to document the experimental procedure and perform preliminary plausibility checks on the measured data. First results demonstrate that system response data and environmental conditions are recorded reliably and that environmental effects significantly affect the long-term measurements. Therefore, a suitable data set is provided as open-source data for future studies on data normalization and automated damage detection.

**Keywords** structural health monitoring; load test; ambient excitation; environmental effects; data acquisition; damage detection; mobile sensing system; plausibility checks

## 1 Introduction

Structural health monitoring is the continuous observation of engineering structures and the actions acting on them to detect damage and predict future performance. Unlike inspections at regular intervals, which allow only visual damage present at a given time to be detected, structural health monitoring provides a continuous flow of information about the condition of the structure and possible hidden damage. Many damage mechanisms initiate on material level and slowly develop over component level to safety critical damages that affect the global structure. However, sudden failures during extreme events (floods, storms, earthquakes, etc.) or changes in prestress and support conditions can quickly lead to safety critical states and limited serviceability, as they lead to extreme stresses and safety critical deformations on roadways and railways. Scour, i. e., the washing

out of bridge foundations in rivers and coastal areas, and subsequent pier settlements or rotations are known to be the main cause for bridge collapses [1], and the 2021 flood catastrophe in Germany highlighted this issue.

One of the main challenges in the development of sensor-based damage detection is the lack of data from structures with well-defined damages, making it difficult to validate new approaches in the research and development stage. Moreover, a large amount of data has to be available from the undamaged state to train machine learning algorithms and remove the effect of environmental and operational variables, such as temperature variations. Ideally, one or two seasonal cycles have to be captured, but most academic studies are limited to a few measurement days, measurement quantities, or exhibit inadequate long-term stability. For example, the I-40 Bridge [2] in the United States is a pioneering case study in bridge monitoring, where a series of vibration-based tests are conducted in the early 1990s. It is a composite bridge with a concrete deck and two steel girders. The four examined damage scenarios include varying cuts through the web and the flange of the main girder. The experimental campaign includes forced and ambient tests under varying temperature and different loading conditions, but it is limited to few testing days. Another case study is the Alamosa Canyon Bridge [3] in the United States, where vibration-based experiments are conducted to investigate the effect of temperature gradients across the bridge over a 24 h time window. The Z24 Bridge in Switzerland [4,5] might be the most comprehensive case study; it is a post-tensioned concrete box-girder bridge with a main span of 30 m and two side spans of 14 m. The applied damage scenarios include a gradual settlement of the pier (by 20, 40, 80, and 95 mm) as well as a foundation tilt, concrete spalling (affecting an area of 12 and 24 m<sup>2</sup>), a simulated landslide, the failure of tendon anchors (2 and 4 anchor heads), and the rupture of tendons (2, 4, and 6 out of 16). Structural data are recorded over a period of 1 year to examine environmental effects, but the instrumentation is limited to 16 accelerometers. Another prominent benchmark is the S101 Bridge in Austria [6], where a series of vibration tests are conducted on the three-span concrete bridge before its premature demolition. Three major damages were applied: a cut through the pillar, a gradual settlement of the damaged pillar in three steps up to 2.7 cm (where an auxiliary structure is attached to the pillar to impose the support settlement), and a cut through four internal prestressing tendons. The data sets were collected over a period of 4 days, which might not be adequate to study the effect of environmental conditions.

The goal of this article is to add another benchmark study for bridge monitoring, which contains well-defined damage states and a long-term measurement from the undamaged structure. Different static and dynamic response quantities

This is an open access article under the terms of the Creative Commons Attribution-NonCommercial License, which permits use, distribution and reproduction in any medium, provided the original work is properly cited and is not used for commercial purposes.

are recorded (such as accelerations, inclinations, strains, and forces), and preliminary checks are performed to ensure that the data are plausible and suited for future studies on data normalization (i.e., the automated removal of environmental conditions) and damage detection. The remaining sections are organized as follows: Section 2 describes the test bridge and the experimental setup. Section 3 presents the results of a preliminary data analysis and plausibility checks. Section 4 draws some conclusions, and in Section 5, information is given on how to publicly access the measurement data.

## 2 Experiment description

This section describes the entire experiment including the structural system of the examined bridge, the damage scenarios, the instrumentation, and the measurement strategies.

### 2.1 Bridge description

The test bridge is built in 2007 at the University of the Bundeswehr in Munich, Germany. Fig. 1 shows the schematic drawing of the test bridge. It is a steel–concrete composite structure with a length of 30 m, consisting of two primary steel girders (HEB1000), seven transverse braces at axis 2 to 8 (HEB120), and two transverse braces (HEB240) at both abutments. The concrete deck is split into 11 segments of varying length ( $L \times B \times T = 1.4\text{--}3.0 \times 4.0 \times 0.2$  m). The gaps between the concrete segments are filled with partially cracked cement paste. The concrete exhibits a compressive strength C30/37 and the steel material is of grade S235. The

composite effect is achieved through a bolted connection via M24 bolts between the flanges of the longitudinal girders and the inverted T-shaped steel beams that are partially embedded on the lower of the concrete segments. The bolts are arranged at a uniform distance of 50 cm, starting at a distance of 20 cm on either end of the girders. The test bridge exhibits support blocks under the main girders at both abutments and additionally at the middle span. Therefore, the load-bearing system of the test bridge can be converted from a single-span system to a double-span system. To simulate support settlements, a central support is temporarily installed. The installation of the temporary supports is path-controlled and lifted with hydraulic jacks until all supports are level.

### 2.2 Damage scenarios

The applied damage scenarios include a series of failing bolts between steel girders and the concrete, the failure of transverse braces, mass changes on the deck, and even settlements of both middle supports, with more details in the following list.

- *Failing bolts:* This case is simulated by removing bolts between the girders and concrete deck in three selected locations, as show in Fig. 2. The bolts are removed in the locations where maximum shear forces are expected (Case 1 and 3). In addition, the Case 2 is chosen as a comparison to the other cases. For each test, 20 out of 240 bolts are removed on both girders, so 10 bolts at each girder.
- *Failure of transverse braces:* This scenario is applied by successively removing four out of nine transverse beams in three data sets. In the first data set, transverse beam #3 is re-

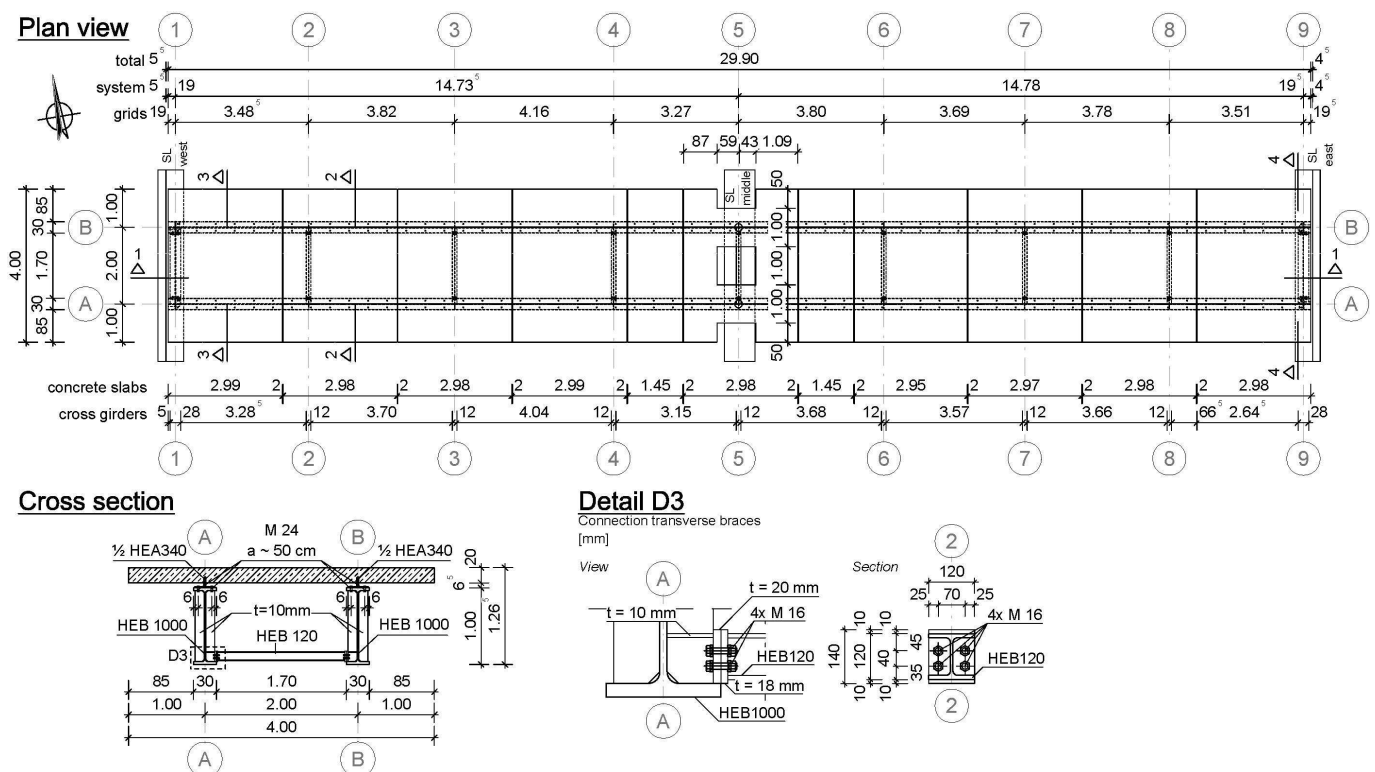


Fig. 1 Schematic drawing of the test bridge at the University of the Bundeswehr Munich

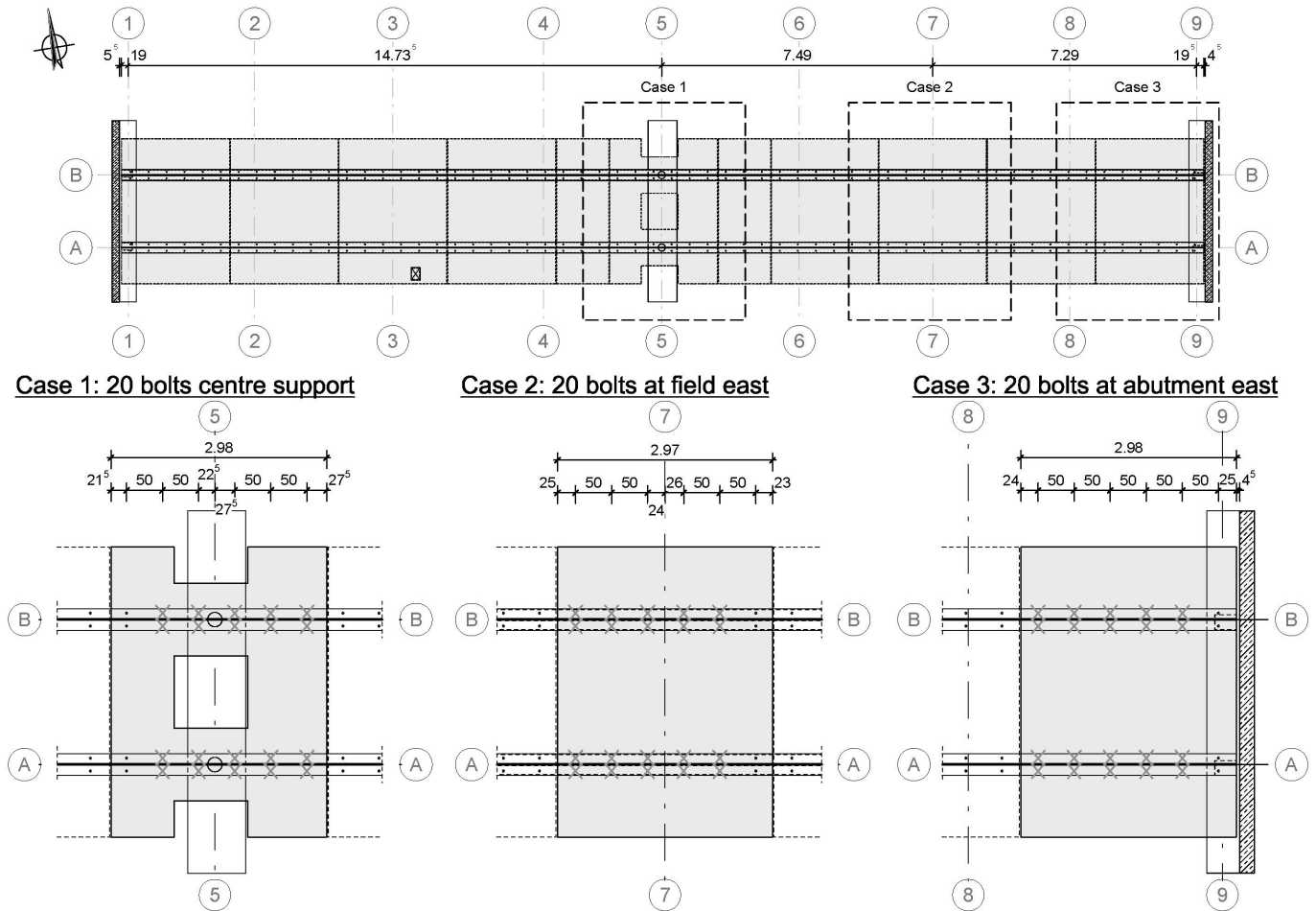


Fig. 2 Failing bolts between steel and concrete

moved. In the second data set, transverse beams #2 and #3 are removed, and ultimately, transverse beams #2, #3, #7, and #8 are removed. The positions of the removed transverse beams are shown in Fig. 3.

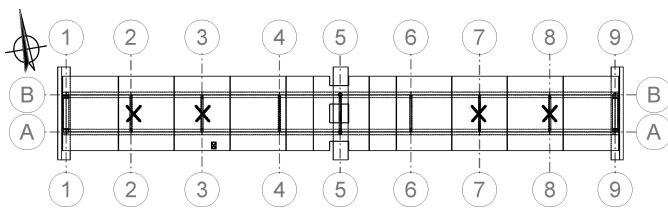


Fig. 3 Failure of transverse braces

- *Mass changes*: This scenario is simulated by adding sandbags with total load of 200 kg and later 400 kg on the bridge deck. The details of the mass changes cases are shown in Fig. 4.
- *Settlements*: This scenario is applied by incrementally lowering the middle supports through mechanical jacks. Firstly, the supports are lowered by 1 cm, then 2 cm, and finally 3 cm. The exact position is controlled by means of inductive displacement sensors and laser distance measurement devices (Disto D8, Leica).

### 2.3 Instrumentation plan

This section summarizes the instrumentation of the bridge in Tab. 1 and Fig. 5. To measure the bridge vibration, the ac-

Tab. 1 Sensor specifications

Sensors	Type/model	Quantity [pcs]	Sampling rate	Mounting
Uniaxial accelerometer	Metra KS48 C	8	1000 Hz	Magnetic mount
Triaxial accelerometer	Metra KS823B	8	1000 Hz	Magnetic mount
Uniaxial inclinometer	Seika SB1 U	10	100 Hz	Screw clamp fastening
Strain gauge (full Wheatstone bridge)	HBM 6/120ALY11	6	100 Hz	Adhesive mount
Load cell	Novatech F204, Alhen ALF204	2	1 and 1000 Hz	
(Wind angle and speed, air temperature, relative humidity, solar radiation)	Lambrech meteo u[sonic]WS7	1	1 Hz	
USB camera for load tests		1	5 fps	

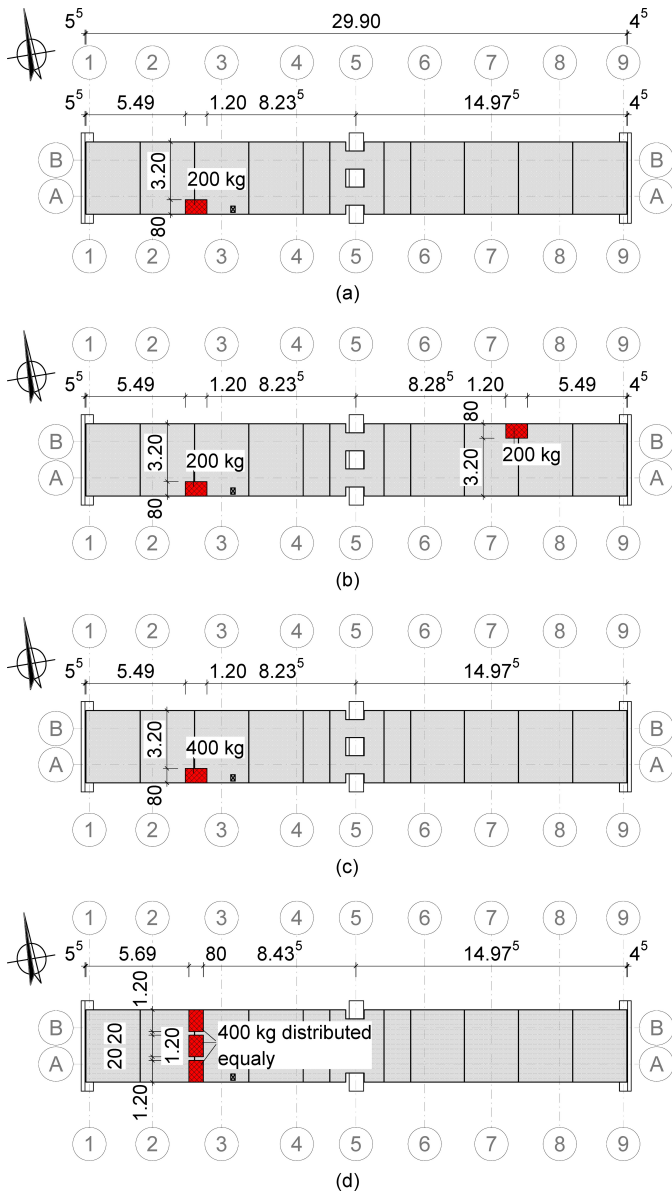


**Fig. 4** Mass changes: a) 200 kg as a point load, b) 2 × 200 kg as point loads on opposite sides, c) 400 kg as a point load, and d) 400 kg as a line load

celerometers are mounted in the centreline of the beam and under the bottom flanges of the steel girders. The uniaxial sensors with a nominal sensitivity of 100 mV/g are placed under the South girder, while the triaxial sensors with a nominal sensitivity of 500 mV/g are placed on the North girder. The rotation of the bridge in the longitudinal and transverse directions is measured with inclinometers, which are placed along the main girders and the transverse braces, respectively. Strain gauges are placed in locations of maximum strains, i.e., the main girder's top flange (outer side) over the middle supports, and centrally at the main girder's midspan. To measure reaction forces at the middle supports, load cells are installed. A shaker with a total weight of 140 kg replaces traffic loads and injects white noise vertically into the bridge, with a frequency bandwidth between 2 and 100 Hz and a maximum acceleration of 1.5 m/s<sup>2</sup>. More details regarding the sensor placement can be found in Tab. 1 and Fig. 5.

## 2.4 Measurement strategy

The measurement data are organized into short-term measurements and one long-term measurement (18 days). Firstly, the short-term tests are conducted, where each damage scenario from Section 2.2 is applied. Each short-term test contains a dynamic load test of 12 min length and an ambient vibration test with a duration more than 3 h. Secondly, a long-term measurement is conducted in the reference state and under varying environmental conditions. Finally, the support settlement is applied, as it would be challenging to restore the exact same support conditions afterwards. The experiment is conducted from 4 March 2022 until 11 April 2022 with a short interruption after the long-term test and a detailed timeline shown in Tab. 2. During the 12 min load test, a truck with 2300 kg is driven across the bridge from West to East and back (Fig. 6). Afterwards, the truck is parked in three parking positions for 120 s, i.e., in the centre span West, over the middle support, and the centre span East. The load tests are recorded using a CCTV camera, and all other events are recorded in the measurement logbook.

## 3 Data plausibility checks

This section presents the results of the preliminary data analysis. Plausibility checks are performed for short- and long-term measurements, but no in-depth damage detection studies are shown. The goal is to demonstrate that data are recorded reliably and that it can be used for future studies related to data normalization (the removal of environmental effects) and automated damage detection and localization.

### 3.1 Short-term measurements

#### 3.1.1 Undamaged state

##### Vibrations

For vibration data, the plausibility checks are performed by running a series of operational modal analyses (OMAs). Before doing that, the quality of the vibration signal is verified by checking it for spikes, dropouts, clipping, long-term drifts, and verifying the normal distribution assumption. Covariance-driven subspace system identification (SS-Cov) [7] is used to estimate the modes of vibration including natural frequencies, damping ratios, and mode shapes. The OMA is conducted in combination with an automated clustering and mode tracking algorithm [8]. A typical stabilization diagram is shown in Fig. 7 with the corresponding mode of vibration in Fig. 8. The signal-to-noise ratio (SNR) can also be estimated from power spectral density (PSD) plotted on a dB scale. According to Brincker and Ventura [9], the SNR of OMA applications can be estimated as the distance between the peaks in the PSD and the noise level, that is, the level at which the singular values cannot be distinguished any more. The SNR of the vibration measurement is approximately 70 dB, which is considered an excellent SNR. The result of the analysis shows that the vibration modes are closely spaced,

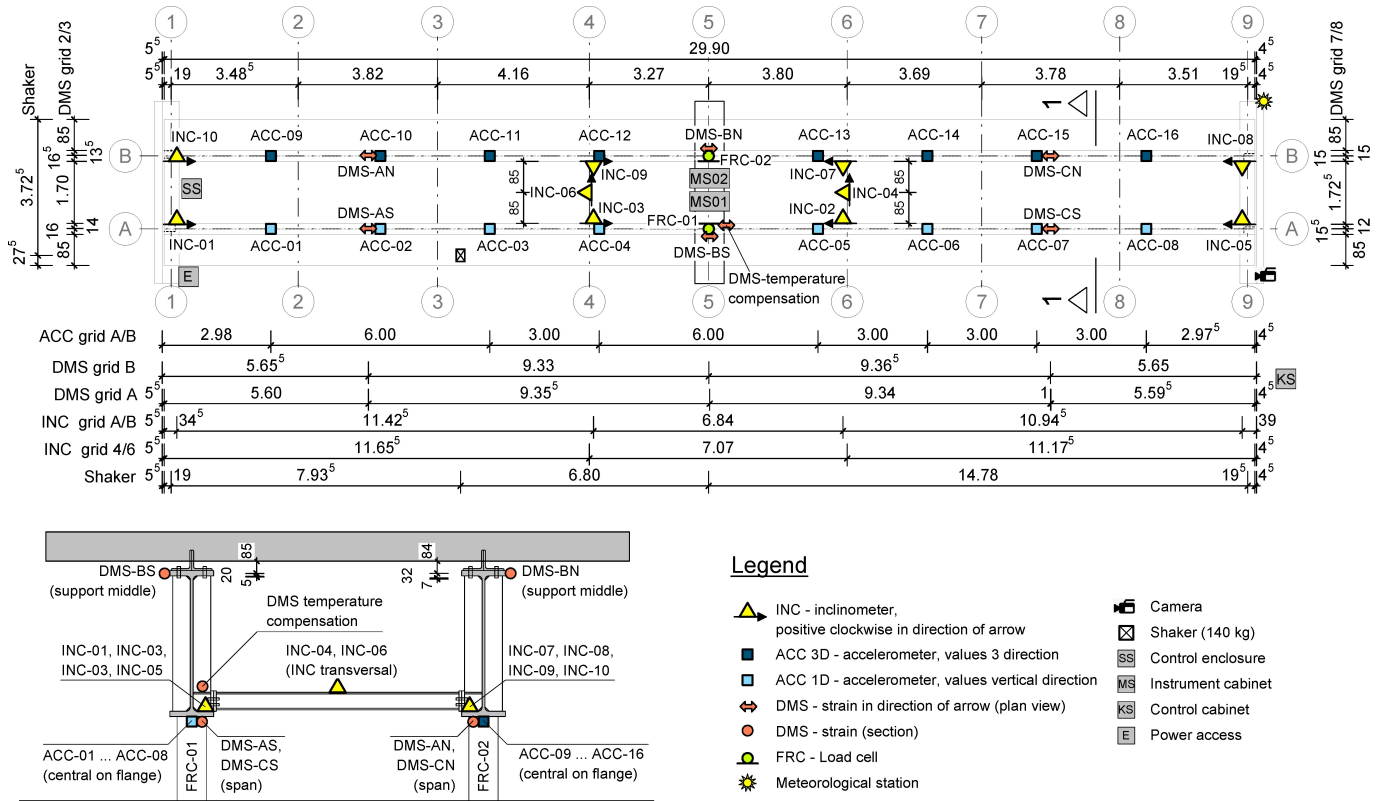


Fig. 5 Instrumentation plan

Tab. 2 Timeline of the experiment

Date	Measurement strategy	Measurement approach			Remark
		Load test	Ambient measurement Short-term	Long-term	
2022-03-04	Installation of measurement system				
2022-03-07	<b>Reference state</b>	X	X		
2022-09-08	Failing bolts over middle supports	X	X		
2022-03-08	Failing bolts at eastern midspan	X	X		
2022-03-08	Failing bolts at western abutment	X	X		Overnight
2022-03-09	<b>Reference state</b>	X			
2022-03-09	Removal of transverse beam #3	X	X		
2022-03-09	Removal of transverse beams #2 and #3	X	X		
2022-03-09	Removal of transverse beams #2, #3, #7, and #8	X	X		Overnight
2022-03-10	<b>Reference state</b>	X			
2022-03-10	200 kg as point load	X	X		
2022-03-10	200 kg + 200 kg as point loads	X	X		
2022-03-10	400 kg as point load	X	X		Overnight
2022-03-11	400 kg as line load	X	X		
2022-03-11	<b>Reference state</b>			X	18 days record
2022-04-11	<b>Reference state</b>	X			
2022-04-11	1 cm settlement	X	X		
2022-04-11	2 cm settlement	X	X		
2022-04-11	3 cm settlement	X	X		Overnight

i. e., the natural frequencies are very close to each other due to the double symmetry of the structure. This is especially true for the first vertical mode (9.336 Hz) and the first torsional vibration mode (9.541 Hz). The first and second verti-

cal modes also exhibit a low damping ratio far below 1% if the concrete segments are not activated.



Fig. 6 a) Vehicle for load tests and b) the test bridge as seen from the abutment West

*Inclinations*

Moving forward to the inclinometer data, Fig. 9a shows a representative inclination measurement (INC01 at West abutment) superimposed with the force measurement from sensors FRC-01 and FRC-02. At first glance, the data do not seem plausible, as the high-frequency components mask the static motion of the bridge. This is most likely due to the high resolution and sensitivity of the inclination sensors, which are sufficient to capture the dynamic response. The inclination sensors that are used are statically operating acceleration sensors, which are applied for measuring inclinations in small angular ranges. The sensors have a sensitivity of  $0.20 \text{ V}/^\circ$  and can capture the change of inclination smaller than  $0.001^\circ$ . To remedy this, a digital low-pass filter with a cutoff frequency of 0.2 Hz is applied. By inspecting the filtered signal in Fig. 9b, the two peaks during the crossing become visible, and three plateaus form while the car is in parking position. In addition, the Fast Fourier Transformation (FFT) analysis is performed for the inclinometer data in the ambient measurement. The FFT analysis of inclinometer data leads to the same frequency peaks that form based on vibration data. All inclination records are visually checked and show a similar trend, which completes the plausibility checks.

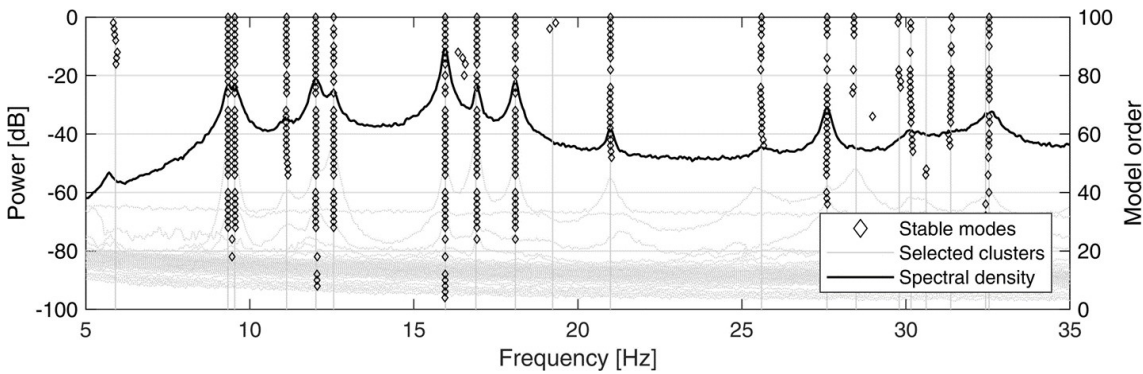
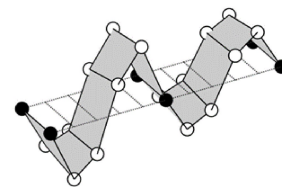
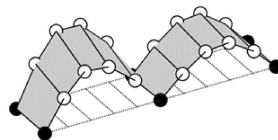
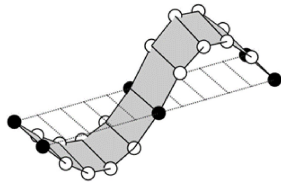


Fig. 7 Stabilization diagram

$f = 9.336 \text{ Hz } \zeta = 0.67\%$

$f = 12.559 \text{ Hz } \zeta = 0.76\%$

$f = 31.368 \text{ Hz } \zeta = 2.11\%$



$f = 9.541 \text{ Hz } \zeta = 1.02\%$

$f = 12.017 \text{ Hz } \zeta = 1.05\%$

$f = 32.429 \text{ Hz } \zeta = 1.00\%$

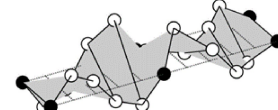
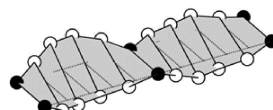
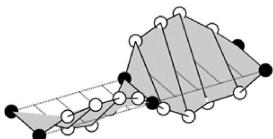
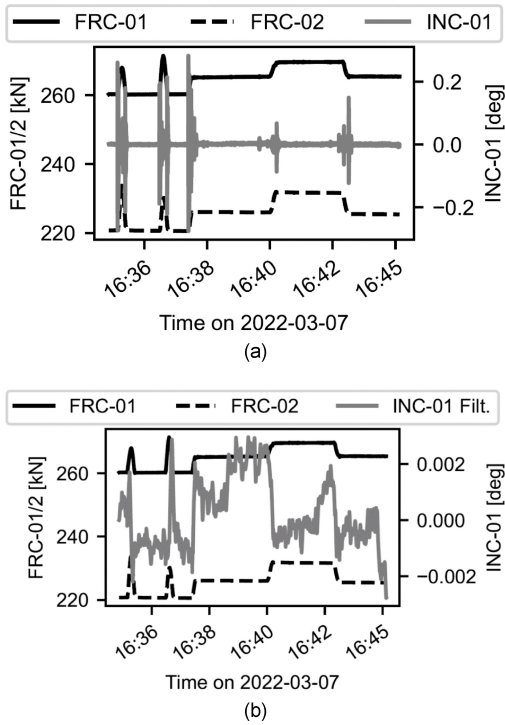


Fig. 8 Global vertical and torsional modes of vibration



**Fig. 9** a) Time history of middle supports reaction and INC01; b) inclination data INC01 after digital filtering

*Support forces*

Figure 10 shows a representative force signal during the load test, recorded at the middle supports of the bridge. The first two peaks represent the moving vehicle, as it passes over the two bridge spans, and the three plateaus represent the static vehicle in the three parking positions (see Section 2.4). It can be seen in the graph that the initial forces measured through the two sensors do not show the same value. This can be explained by the fact that the hydraulic forces are not exactly the same during lifting, as the premise was to level the bridge. When the vehicle passes over the bridge, the two force sensors do not show the exact same amplitude because the vehicle slightly deviated from the central axis. When parked over the middle support, the total load registered by two force sensors is about 20 kN. This is equivalent to about 89% of the vehicle’s weight. This value is 10% less than expected based on the structural analysis, and the deviation could be explained by the fact that the middle supports are less stiff than the bearings at abutments and act as some sort of spring during loading.

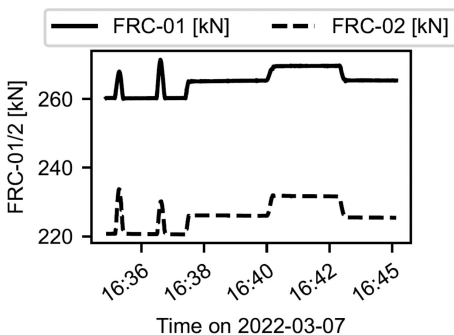


**Fig. 10** Time history of support forces

*Strains*

Figure 11 shows a comparison between strain measurements (sensor DMS\_CN) and force measurements of sensor FRC-01 and FRC-02 on 7 March 2022. The peaks in the strain measurements align with the peaks of the force measurements. The amplitude of the strain readings in parking position three has a similar value as the amplitude while the vehicle is moving across the bridge, which is also to be expected. All strain and force readings are visually inspected and show a similar result, which concludes the plausibility checks.

**3.1.2 Damaged states**

*Support forces*

Figure 12 shows the signals of the support forces before and after the support settlement on 11 April 2022. As expected, the support forces decrease as the settlement increases.

*Strains*

Figure 13 shows the evolution of the strain measurements at sensor DMS\_CN at the lower web of the main girder (at midspan). The plots visualize four load tests, two ambient data sets, and the lowering of the middle supports in three phases. The strain magnitude after unloading increases from 0 to 34.5  $\mu\text{m/m}$ , then to 85.4  $\mu\text{m/m}$ , and finally to 131  $\mu\text{m/m}$  due to the incremental lowering of the middle supports by 1, 2, and 3 cm, respectively. The influence of temperature can be clearly seen in the strain signal during the ambient measurements from 9:30 to 13:40 and from 13:50 to 17:40, highlighting the need for a proper temperature compensation. However, in this article, the compensation for environmental influences is not analysed. This plausibility check is performed for all other strain sensors, which showed a similar result and indicated a reliable data acquisition.

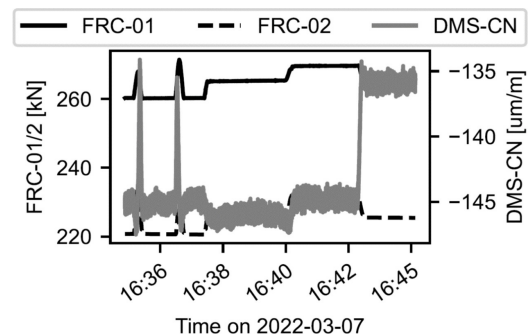


**Fig. 11** Time history of support forces and strain DMS\_CN

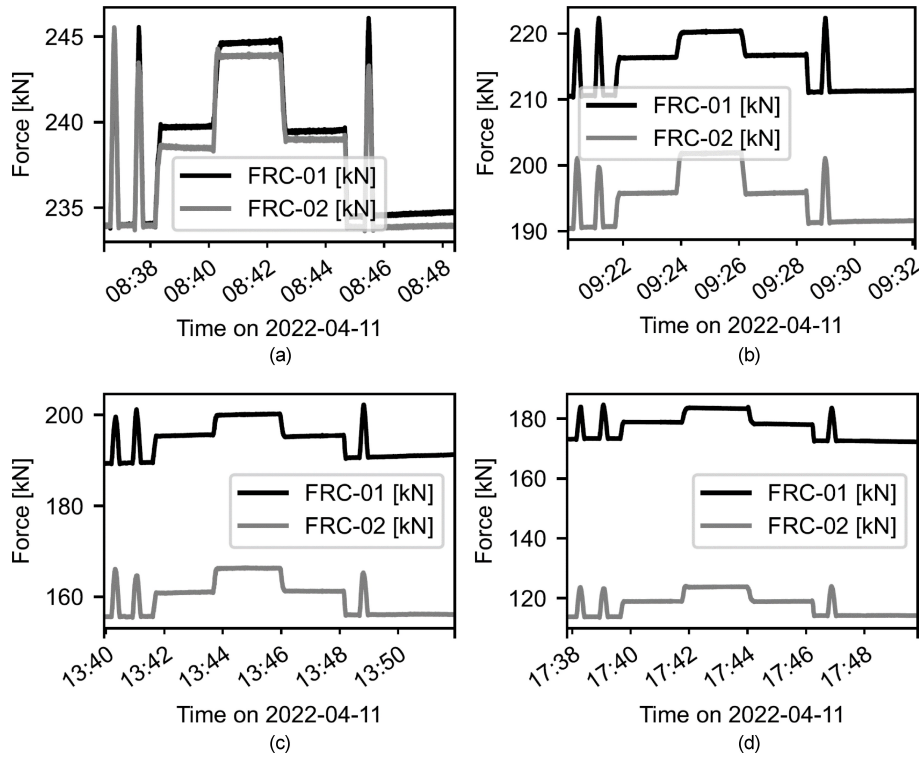


Fig. 12 Time history of support forces: a) reference state, b) 1 cm settlement, c) 2 cm settlement, and d) 3 cm settlement

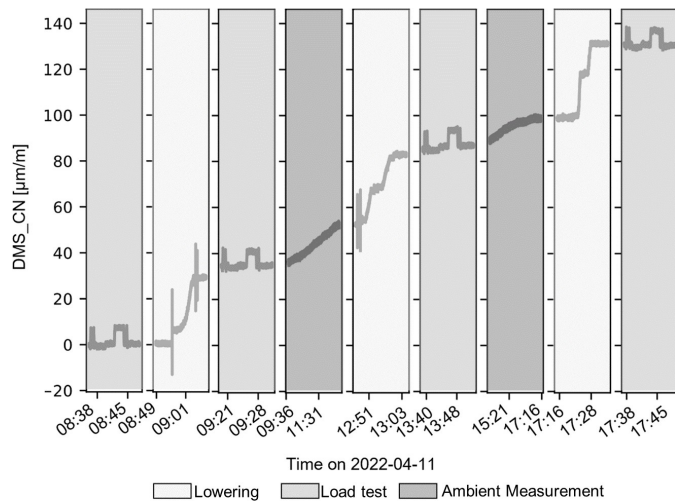


Fig. 13 Strain measurement history of sensor DMS\_CN

### 3.2 Long-term measurements

#### Vibration data

OMA is also performed for long-term vibration data. As shown in Fig. 14, the natural frequencies change due to daily temperature changes between  $-4$  and  $+20$  °C. Fig. 15 shows the Histogram of OMA of the natural frequencies of the first four vibration modes in the reference state and the four damage states. The plots verify that the vibration data are recorded reliably and that the system response quantities are affected by temperature variations. Therefore, the measurement data are appropriate for future studies related to data normalization, i.e., the removal of environmental effects.

#### Weather station

The ambient air temperature is comparable to the data recorded at the nearby weather station at Munich Airport (Fig. 16). For the other environmental parameters such as wind speed and direction, it is challenging to verify the data, as the local terrain significantly influences the measurements.

## 4 Conclusion

The main contribution of this article is the creation of a benchmark data set for bridge monitoring in combination with a detailed experiment description. The examined damage scenarios include a support settlement by 1, 2, and 3 cm, as well as the failure of transverse braces, the failure of bolts between steel and concrete, and the application of extra masses. Extra masses are included as they might be an appropriate means to perform non-destructive quality control checks on Structural Health Monitoring (SHM) System. The premise was to create a data set with well-defined damage scenarios and a sufficiently long data set for data normalization studies (the removal of environmental and operational conditions). In general, the jump from laboratory experiments to real bridges is large because of sudden variations in excitation, environmental conditions, and other challenge disturbances. This study on the test bridge is an intermediate step between laboratory experiment (controlled load and environment) and the real bridge experiment (uncontrolled load and environment). The test bridge is exposed to real environmental condition and not exposed to real traffic. However, under constant shaker excitation, there are no sudden variations in the excitation. This means



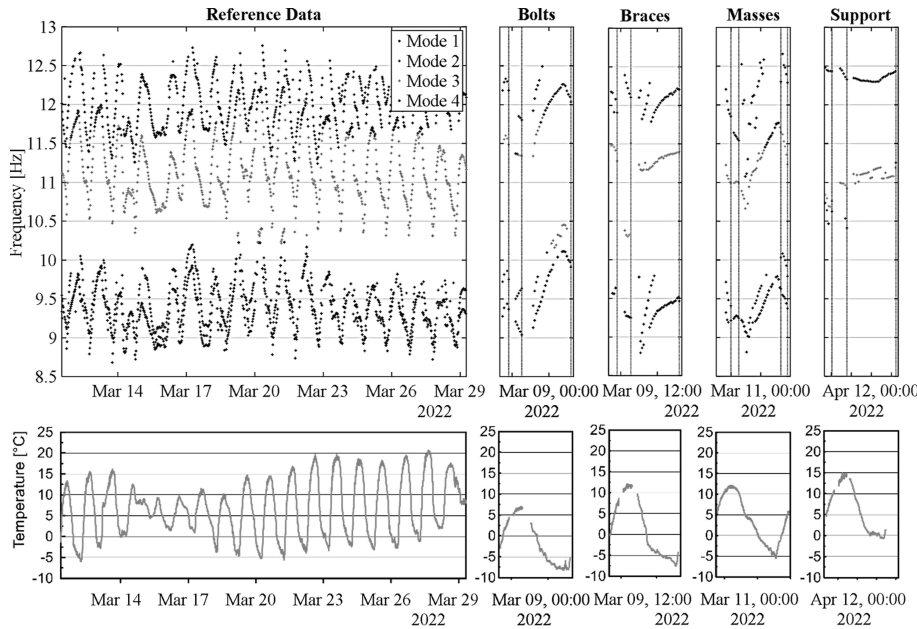


**Fig. 14** Natural frequencies of the first four modes of vibration in the reference state (left), the four damage states (right), and air and its respective temperature (below)

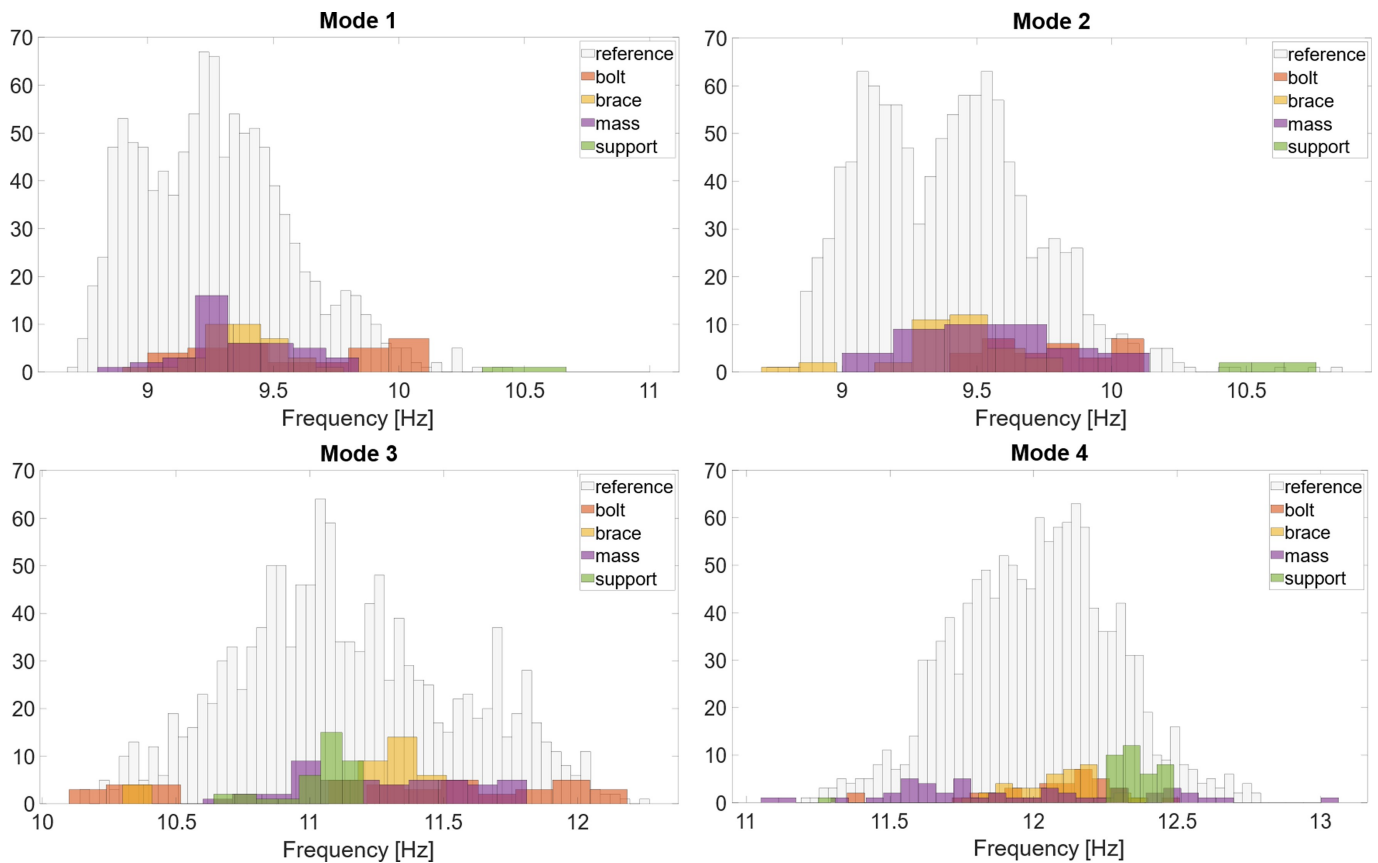


**Fig. 15** Histogram of the natural frequencies of the first four vibration modes in the reference state and the four damage states

that this study may be valuable for training or establishing an algorithm that compensates for fluctuating environmental conditions but not for fluctuating excitation. The results from preliminary data analysis showed that the data are recorded reliably and appropriate for future studies related to data normalization and automated damage detection algorithms.

### Acknowledgements

This research was funded by dtcc.bw – Digitalization and Technology Research Center of the Bundeswehr [projects SHM, RISK.twin, MISDRO]. Dtcc.bw was funded by the European Union – NextGenerationEU. The collaboration partners at the Helmut-Schmidt University/University of the Bundeswehr Hamburg, the University of the Bundeswehr Munich, and the Technical University of Munich are gratefully ac-

knowledge. Open Access funding enabled and organized by Projekt DEAL.

### Data Availability Statement

MATLAB and Python routines to preprocess the exported raw data in CSV and to generate many of the presented plots are publicly available at <https://github.com/imcs-compsim/munich-bridge-data> and can be searched using the search keywords ‘Munich bridge data’. The repository also contains sample measurement data from each sensor type (acceleration, strain, force, and inclination) for one load test on 2022-04-11, sampled at 100 Hz and Finite Element Model in Ansys. The

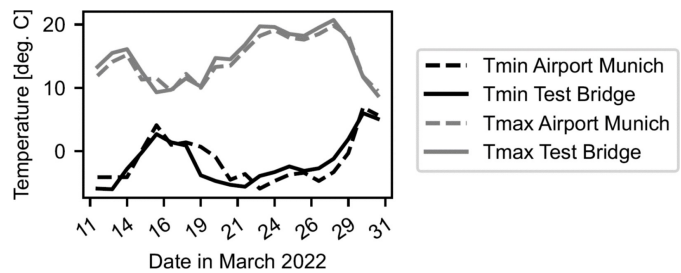


Fig. 16 The measured ambient air temperature in comparison to Munich Airport

full data set in CSV and DXD format (3 TB) and technical drawings can be obtained upon request from the authors.

### References

- [1] Shirole, A. M.; Holt, R. C. (1991) *Planning for a comprehensive bridge safety assurance program*. Transportation Research Record 1290, pp. 39–50.
- [2] Farrar, C. R.; Baker, W. E.; Bell, T. M.; Cone, K. M.; Darling, T. W.; Duffey, T. A.; Eklund, A.; Migliori, A. (1994) *Dynamic Characterization and Damage Detection in the I-40 Bridge over the Rio Grande (No. LA-12767-MS)*. Los Alamos, NM: Los Alamos National Lab.
- [3] Farrar, C. R.; Cornwell, P. J.; Doebling, S. W.; Prime, M. B. (2000) *Structural Health Monitoring Studies of the Alamosa Canyon and I-40 Bridges (No. LA-13635-MS)*. Los Alamos, NM: Los Alamos National Lab. (LANL).
- [4] Krämer, C.; De Smet, C. A. M.; De Roeck, G. (1999) *Z24 bridge damage detection tests*. IMAC 17, the International Modal Analysis Conference, Vol. 3727. Florida, Society of Photo-optical Instrumentation Engineers, pp. 1023–1029.
- [5] Maeck, J.; De Roeck, G. (2003) *Description of Z24 benchmark*. Mechanical Systems and Signal Processing 17, No. 1, pp. 127–131.
- [6] Wenzel, H.; Veit-Egerer, R.; Widmann, M. (2013) *Case Study: S101 in: Wenzel, H. (ed.) Industrial Safety and Life Cycle Engineering: Technologies, Standards, Applications*. VCE Vienna Consulting Engineers ZT GmbH
- [7] Van Overschee, P.; De Moor, B. L. (2012) *Subspace Identification for Linear Systems: Theory – Implementation – Applications*. Boston, US: Springer Science & Business Media.
- [8] Mendler, A.; Ventura, C. E.; Nandimandalam, L.; Kaya, Y. (2020) *Launching Semi-automated modal identification of the Port Mann Bridge*. Dynamics of Civil Structures. Cham: Springer, Vol. 2, pp. 269–280.
- [9] Brincker, R.; Ventura, C. (2015) *Introduction to Operational Modal Analysis*. Chichester, West Sussex UK: John Wiley & Sons.

### Authors

Yogi Jaelani, M.Sc. (corresponding author)  
 yogi.jaelani@hsu-hh.de  
 Helmut-Schmidt University/University of the Bundeswehr Hamburg  
 Chair of Engineering Material and Building Preservation  
 Holstenhofweg 85  
 22043 Hamburg, Germany

Alina Klemm, M.Eng.  
 alina.klemm@hsu-hh.de  
 Helmut-Schmidt University/University of the Bundeswehr Hamburg  
 Chair of Steel Construction  
 Holstenhofweg 85  
 22043 Hamburg, Germany

Johannes Wimmer, M.Sc.  
 koehncm@hsu-hh.de  
 Helmut-Schmidt University/University of the Bundeswehr Hamburg  
 Chair of Engineering Material and Building Preservation  
 Holstenhofweg 85  
 22043 Hamburg, Germany

Fabian Seitz, M.Sc.  
 johannes.wimmer@unibw.de  
 University of the Bundeswehr Munich  
 Institute for Structural Engineering  
 85577 Neubiberg, Germany

Martin Köhncke, M.Sc.  
 fabian.seitz@unibw.de  
 University of the Bundeswehr Munich  
 Institute for Structural Engineering  
 85577 Neubiberg, Germany

Dr.-Ing. Francesca Marsili  
 marsilif@hsu-hh.de  
 Helmut-Schmidt University/University of the Bundeswehr Hamburg  
 Chair of Engineering Material and Building Preservation  
 Holstenhofweg 85  
 22043 Hamburg, Germany

Alexander Mendler, Ph.D.  
 alexander.mendler@tum.de  
 Technical University of Munich  
 TUM School of Engineering and Design  
 Chair of Non-destructive Testing  
 Franz-Langinger-Straße 10  
 81245 München, Germany

Dr.-Ing. Max von Danwitz  
 max.danwitz@unibw.de  
 University of the Bundeswehr Munich  
 Institute for Mathematics and Computer-Based Simulation (IMCS)  
 85577 Neubiberg, Germany

Prof. Dr.-Ing. habil. Sascha Henke  
sascha.henke@hsu-hh.de  
Helmut-Schmidt University/ University of the Bundeswehr Hamburg  
Chair of Geotechnical Engineering  
Holstenhofweg 85  
22043 Hamburg, Germany

Prof. Dr.-Ing. Max Gündel  
guendelm@hsu-hh.de  
Helmut-Schmidt University/ University of the Bundeswehr Hamburg  
Chair of Steel Construction  
Holstenhofweg 85  
22043 Hamburg, Germany

Prof. Dr.-Ing. Thomas Braml  
thomas.braml@unibw.de  
University of the Bundeswehr Munich  
Institute for Structural Engineering  
85577 Neubiberg, Germany

Prof. Dr.-Ing. Max Spannaus  
max.spannaus@unibw.de  
University of the Bundeswehr Munich  
Institute for Structural Engineering  
85577 Neubiberg, Germany

Prof. Dr.-Ing. Alexander Popp  
alexander.popp@unibw.de  
University of the Bundeswehr Munich  
Institute for Mathematics and Computer-Based Simulation (IMCS)  
85577 Neubiberg, Germany

Prof. Dr.-Ing. Sylvia Keßler  
sylvia.kessler@hsu-hh.de  
Helmut-Schmidt University/ University of the Bundeswehr Hamburg  
Chair of Engineering Material and Building Preservation  
Holstenhofweg 85  
22043 Hamburg, Germany

#### How to Cite this Paper

Jaelani, Y.; Klemm, A.; Wimmer, J.; Seitz, F.; Köhncke, M.; Marsili, F.; Mendler, A.; von Danwitz, M.; Henke, S.; Gündel, M.; Braml, T.; Spannaus, M.; Popp, A.; Keßler, S. (2023) *Developing a benchmark study for bridge monitoring*. Steel Construction 16, No. 4, pp. 215–225.  
<https://doi.org/10.1002/stco.202200037>

This paper has been peer reviewed. Submitted: 02. November 2022; accepted: 15. May 2023.